Aerosol and Air Quality Research, 14: 515–521, 2014
Copyright © Taiwan Association for Aerosol Research
ISSN: 1680-8584 print / 2071-1409 online
doi: 10.4209/aaqr.2013.06.0227

Hydrogen Bonded Pyridine Dimer: A Possible Intermediate in the Electrocatalytic Reduction of Carbon Dioxide to Methanol

Yong Yan, Jing Gu, Andrew B. Bocarsly[*]

Frick Laboratory, Department of Chemistry, Princeton University, Princeton, NJ 08544, USA

ABSTRACT

Previously, electrogenerated pyridinyl was implicated as a catalyst for the reduction of CO_2 to methanol. However, recent quantum mechanical calculations of both the homogeneous redox potential for the pyridinium/pyridinyl redox couple (900 mV more negative than experimentally reported) and the pK_a of the reduced pyridinyl species (~27) have led to the proposal that the homogeneous reduction of pyridinium does not play a role in the observed catalytic reduction of CO_2 to methanol. In contrast, a more complete consideration of the reaction including the realization that pyridinium reduction is tightly coupled to H_2 evolution, produces a calculated redox potential in agreement with the experimental findings. In reexamining this system, it is found that aqueous solutions containing a near equimolar mixture of pyridine and pyridinium (i.e., solution pH near the pyridinium $pK_a = 5.2$) contain a substantial concentration of a hydrogen-bonded dimer formed by the generation of a N-H···N bond containing one strong NH bond and one elongated NH bond. This species has been identified by X-ray diffraction of crystals grown in aqueous media from pyridine/pyridinium mixtures, and can be observed directly in solution using Raman spectroscopy. DFT (density functional theory) calculations indicate that the pK_a for this species is ~22, a value that is consistent with a proton exchange capability. This suggests that this hydrogen bonded dimer may be the pre-electrocatalyst for the observed activation of CO_2.

Keywords: CO_2 sequestration and conversion; Catalyst; Electrochemistry; Pyridinium.

INTRODUCTION

An accumulation of carbon dioxide in the atmosphere, from a concentration of 270 ppm before the industrial revolution to 400 ppm today has led to concern about the long term affects of this change (NOAA, 2013). It is now widely reported that anthropogenic CO_2, due to its role as a greenhouse gas, is the major contributor to climate change (Albo *et al.*, 2010). A feasible and economical route to recycling environmentally deleterious CO_2 emissions back to valuable industry feedstock or to fuels is urgently needed (Aresta, 2010).

Our group has reported that a pyridine catalyst in aqueous solution can electrocatalytically reduce CO_2 to methanol with very low overpotential on a platinum electrode (Seshadri *et al.*, 1994; Cole *et al.*, 2010). Recently, an eloquent calculation by Keith and Carter (Keith and Carter, 2012) provided computational access to the pK_a of short-lived pyridinyl species formed via electroreduction of various substituted pyridiniums in aqueous solution [Scheme 1(a), 1(b)]. A knowledge of the physical properties of these molecular species and specifically their acid-base properties is of current interest, since these species have been demonstrated to be potent electrocatalysts for the reduction of aqueous CO_2 to methanol and related products: carbon monoxide, formate or formaldehyde (Cole *et al.*, 2010; Keets *et al.*, 2010; Bocarsly *et al.*, 2012; Yan *et al.*, 2013).

We previously suggested that the electrocatalytic mechanism operating in both metal-based and semiconductor-based electrochemical cells for the reduction of CO_2 involved a mediated charge transfer process in which pyridinium is first reduced at an electrode surface via a one electron charge transfer process, followed by reaction of the electrogenerated pyridinyl species with CO_2 to form a carbamate radical adduct (Scheme 1) (Cole *et al.*, 2010; Morris *et al.*, 2011).

Further reduction of the carbamate produces formate, which in a follow up series of pyridinyl mediated charge transfers goes on to generate methanol. In part, the Keith-Carter calculations are important because they provide access to the pK_as of the pyrdinyl species shown on the left hand side of Eq. (1c). We previously hypothesized that this reaction involved proton loss followed by nucleophilic attack of the pyridinyl on CO_2. Thus, the ability to lose the pyridinyl's nitrogen proton as measured by the pK_a is a critical parameter. However, Keith and Carter found the

---

[*] Corresponding author.
Tel.: 1-609-258-3888; Fax: 1-609-258-2383
E-mail address: bocarsly@princeton.edu

pK_a of the transient pyridinyl (R = H) to be ~27, and thus the proton is not exchangeable. This finding may rule out the proposed mechanism associated with reaction 1(c).

In re-evaluating our findings we now suggest that the observed electrochemistry may derive from the hydrogen bonded pyridinium-pyridine dimer $[py\text{-}H\text{-}py]^+$ shown in Scheme 2.

The Keith-Carter calculational methodology indicates a pK_a for the one electron reduced product of this species of 22. The K_a of the reduced hydrogen bonded dimer is therefore 5 orders of magnitude greater than the K_a of pyridinyl. While still not very acidic, this pK_a does allow for a modest hydrogen exchange rate in aqueous solution (Amyes *et al.*, 2004), providing the opportunity for reactions 1(c) and 1(d) to occur.

Our prior observation (Seshadri *et al.*, 1994; Barton *et al.*, 2008) that CO_2 catalysis is optimal when the pH of the solution is near the pyridine/pyridinium pK_a is a primary factor in suggesting the presence of this species, since a near 1:1 ratio of pyridine to pyridinium stoichiometrically optimizes the equilibrium formation of the hydrogen bonded dimer (Scheme 2).

RESULTS AND DISCUSSION

The existence of the pyridine H-bonded dimer [Reaction 2(b)] has been previously demonstrated in organic solvent by vibrational spectroscopy (Tayyari *et al.*, 2010), isotope exchange NMR (Schah-Mohammedi *et al.*, 2000), and single crystal X-ray crystallography (Minshall *et al.*, 1978; Glidewell *et al.*, 1982; Bramme and Zhao, 1995). However, this dimer species has not been studied in aqueous solution. Water, according to Emsley (Emsley, 1980), is a stronger hydrogen bonding molecule than pyridine. Thus, in an aqueous solution (~56 mol/L water) of 0.010 mol/L total pyridine (~0.005 mol/L each of pyridine and pyridinium)

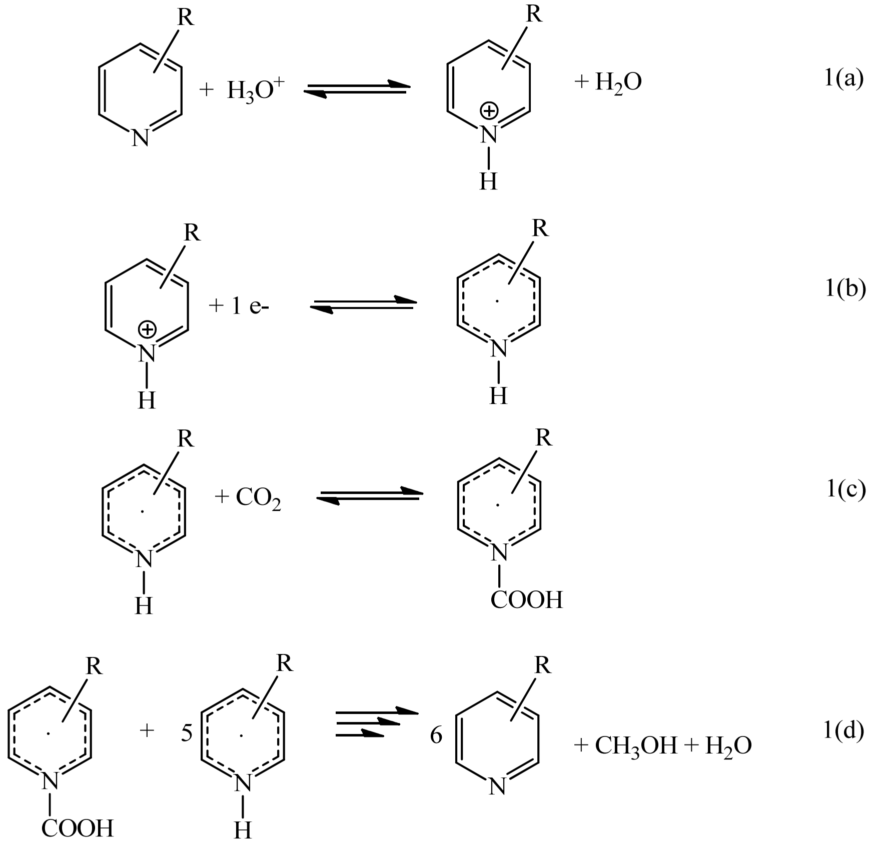

Scheme 1.

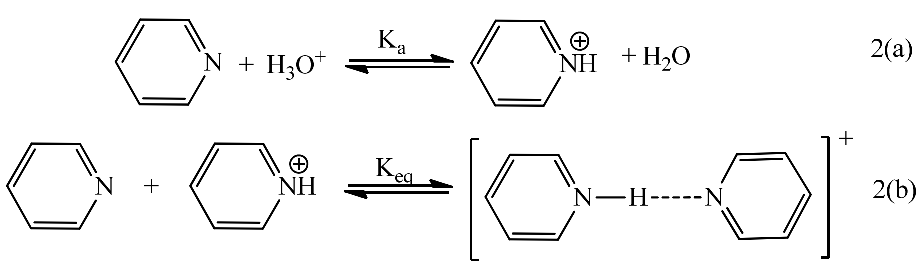

Scheme 2.

the preferred hydrogen bonded species is expected to be the water pyridinium complex: $[\text{py-H-OH}_2]^+$, based both on the concentrations of species present and the hydrogen bonding capability of the solvent. The concentration of the purely pyridine bonded complex $[\text{py-H-py}]^+$ should be negligible. Surprisingly, we find that this latter species is present in relatively high concentration in aqueous electrolyte solution.

In the present study, the presence of the pyridine-pyridinium hydrogen bonded dimer in water was first investigated by addition of equimolar concentrations of pyridine and pyridinium chloride in aqueous solution followed by precipitation of the product by addition of sodium tetraphenylborate. IR spectroscopy of this precipitate matched the reported spectrum of the authentic hydrogen bonded dimer from Tayyari *et al.* (2010) X-ray diffraction quality single crystals of the dimer compound (Fig. 1) were obtained by carefully layering an aqueous solution of 20 mM $NaBPh_4$ with an aqueous solution containing 20 mM pyridinium chloride and 20 mM pyridine. The refined molecular structure produced from this sample was found to be similar to the structure reported by Glidewell. Although the acidic proton position cannot be localized in this structure, the positions of the nitrogen of each ring, which are found to be spaced 2.599 Å apart, is consistent with the existence of a proton between the two pyridyl rings. The symmetry of the structure indicates the proton position on average is at the midpoint of the nitrogen-nitrogen interaction. The 1:1 ratio of tetraphenylborate anions to pyridine dimer moiety demonstrates that the pyridyl dimer is a (1+) cation. Thus, the dimer species must be formed from a neutral pyridine and a pyridinium cation. The N-N distance in several reported pyridine-pyridinium dimer crystals varies from 2.634 Å to 2.745 Å depending on the counterion present (Brammer and Zhao, 1995), suggesting a strong hydrogen bonding interaction between the rings.

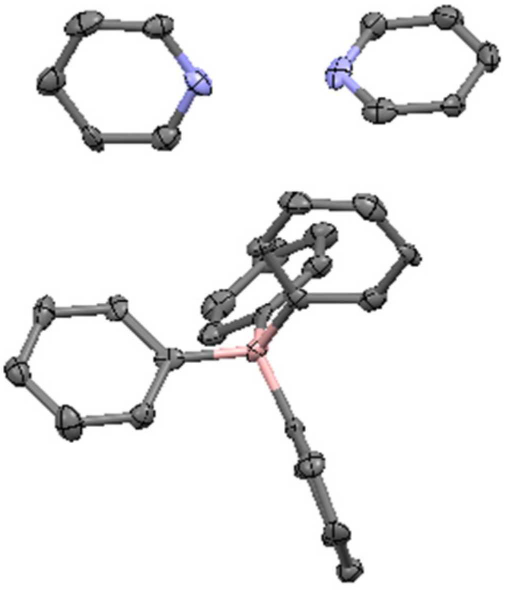

Fig. 1. Crystal structure of pyridinium-pyridine dimer: $[\text{py-H-py}][\text{BPh}_4]$ formed from aqueous solution.

In order to further explore the nature of the dimer hydrogen bond, DFT calculations at the level of the B3LYP/aug-cc-pVDZ basis set and using the CPCM aqueous solvation model were undertaken (Fig. 2). These calculations led to an optimized ground state structure having two orthogonal pyridyl rings and a N-N distance of 2.728 Å, consisting of a short N-H bond and a longer N-H hydrogen bond. Additionally, a local minimum having coplanar pyridyl rings was also obtained, which was only 0.8 kcal/mol higher in energy. In this coplanar geometry the proton is also asymmetrically placed between the nitrogens, which are spaced 2.77 Å apart. In both cases, the N-H bond is significantly lengthened when compared to the N-H bond in pyridinium (1.02 Å), but the N-N distance is shortened compared to the typical N-H-N hydrogen bonded geometry (3 Å) indicating an exceptionally strong interaction (Hamilton and Ibers, 1968). The asymmetric positioning of the proton in both structures is indicative a trapped valence state. Thus, in solution at room temperature it appears that the dimer freely rotates with the hydrogen "on average" being in the nonequilibrium centrosymmetric position. That is, the proton is trapped in a double well potential with a low internal barrier that allows thermal access to both well minima.

Similar quantum calculations were also conducted for the $[\text{py-H-OH}_2]^+$ species, which was previously mentioned to be the expected species in aqueous pyridine solutions. Interestingly, both gas phase and aqueous phase calculations lead to a pyridine dimer compound that is more stable than the pyridine-water hydrogen-bonded complex. As indicated in Table 1, stabilization energies calculated in the gas phase resulted in ca. –7.5 kcal/mol energy preference for the pyridine dimer over the pyridinium-water complex. The calculated energy difference was less obvious in aqueous solution, nevertheless, ca. –3.4 kcal/mol more stabilized energy was obtained for the dimer (–10.5 kcal/mol) over the $[\text{py-H-OH}_2]^+$ species (–7.1 kcal/mol). In order to verify this result we stepwise added hydrogen bonding waters to both the dimer structure and the $[\text{py-H-OH}_2]^+$ structure. We find that after the addition of the first water molecule, further stabilization (within the error of the calculation) is not observed. Thus, a stabilization energy of ca. –3.4 kcal/mol of the dimer over a simple pyridinium hydrogen bonded to water is representative of these structures under conditions

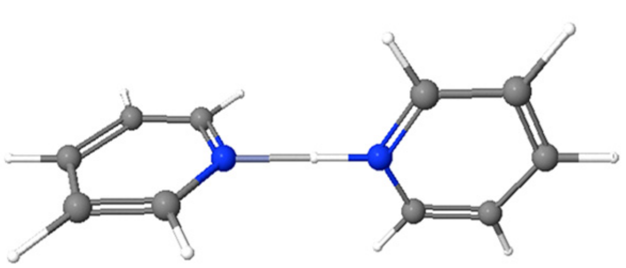

Fig. 2. DFT calculated dimer structure yielding a N---N distance: 2.678 Å (gas phase); 2.728 Å (aqueous CPCM model). The calculated N-H bond length: 1.113 Å (gas), 1.083 Å (aqueous CPCM). (Nitrogen atom: blue; carbon atom: gray; hydrogen atom: white).

Table 1. DFT calculated bond lengths and stabilization energies between water and pyridine forming hydrogen bonds to pyridinium.

DFT/B3LYP/aug-cc-pVDZ	$[py\text{-}H\text{-}py]^+$		$[py\text{-}H\text{-}OH_2]^+$	
	N-H/H-N (Å)	Stabilization energy[a] (kcal/mol)	N-H/H-O (Å)	Stabilization energy[b] (kcal/mol)
gas phase	1.113/1.565	–24.8	1.042/1.709	–17.3
CPCM (aq. model)	1.083/1.645	–10.5	1.045/1.710	–7.1

[a] stabilization energy was calculated as $\Delta H = H[py\text{-}H\text{-}OH_2]^+ - H[pyH]^+ - H[H_2O]$.
[b] stabilization energy was calculated as $\Delta H = H[py\text{-}H\text{-}py]^+ - H\ [pyH]^+ - H[py]$.

where they are fully hydrogen bonded in bulk water. The energy comparisons correlated well with the critical bond lengths. For characteristic stronger hydrogen bonding, as discussed by Emsley (Emsley, 1980), a longer X-H bond, a shorter H-X' bond and a shorter overall X-X' distance should be obtained (where X is the atom chemically bonded to the proton and X' is the hydrogen-bonding partner). The calculated N-H bond length was found to be 0.071 Å longer for the dimer than that for the water hydrogen bonded complex in the gas phase. This is a significant bond lengthening for a N-H bond. Overall, the H-O and H-N bond lengths as well as the N to N and the N to O distances all indicated a stronger hydrogen bonding interaction of the dimer compared to the water containing complex. These DFT calculations provide a rationalization for the experimental observation and isolation of the pyridine dimer species rather than hydrated monomer under our electrochemical conditions.

Total energy calculations, using the optimized dimer geometry, indicate that the dimer is more stable than the sum of pyridinium plus pyridine in water by –10.5 kcal/mol. Based on the crystallographic and molecular structure data there is little doubt that $[py\text{-}H\text{-}py]^+$ exists, and that it can be formed in aqueous solution. The DFT calculated ΔG° for the formation reaction in water, Eq. 2(b), indicates that the reaction is downhill as written by ~ –1.4 kcal/mol. Combination of this value with the measured pyridinium K_a value (Scheme 2), it is predicated that the concentration of $[py\text{-}H\text{-}py]^+$ becomes of the same order of magnitude as the pyridinium concentration for aqueous solutions containing ~1 M pyridine at pH~5.2. Raman spectra taken under these conditions (Fig. 3) clearly show the presence of stretches associated with pyridine, pyridinium and $[py\text{-}H\text{-}py]^+$ based on the reported spectra of authentic samples (Tayyari *et al.*, 2010). Given these results it is certain that the hydrogen-bonded dimer is present under the electrochemical conditions utilized for the catalytic reduction of carbon dioxide.

Further support for the $[py\text{-}H\text{-}py]^+$ dimer as the redox active species is obtained from a digital simulation of cyclic voltammograms obtained for the reduction of pyridine in acidic aqueous solution (pH = 5.2) using the reaction pathway given in Scheme 3. The introduction of reaction 3 is critical to understanding the electrochemical process.

As can be seen in Fig. 4, an excellent match between the simulated and experimental data is obtained. This data fit produces a ΔG for Eq. 2(b) of ~ –3 kcal/mol, reasonably close to the theoretically predicted value noted earlier.

It needs to be noted that a similarly acceptable fit of simulated and real data can be obtained assuming the direct reduction of pyridinium at the electrode. However, the goodness of fit in the current case along with the unambiguous existence of $[py\text{-}H\text{-}py]^+$ in the electrochemical cell leads to the conclusion that the hydrogen bonded dimer must be seriously considered as the primary redox electrocatalyst in our reported reduction of CO_2 to methanol.

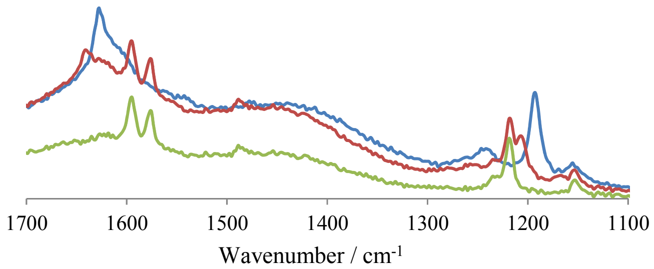

Fig. 3. Raman spectra of pyridinium in water (blue), and an equilibrium mixture of $[py\text{-}H\text{-}py]^+$ and $[pyH]^+$ in water (red). Subtraction of the pure pyridinium spectrum from the mixture spectrum yields the aqueous $[py\text{-}H\text{-}py]^+$ spectrum (green). Unit: cm^{-1}

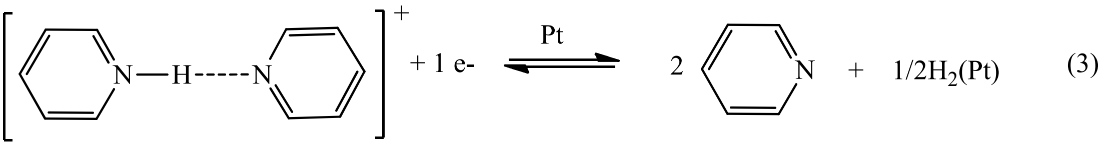

Scheme 3.

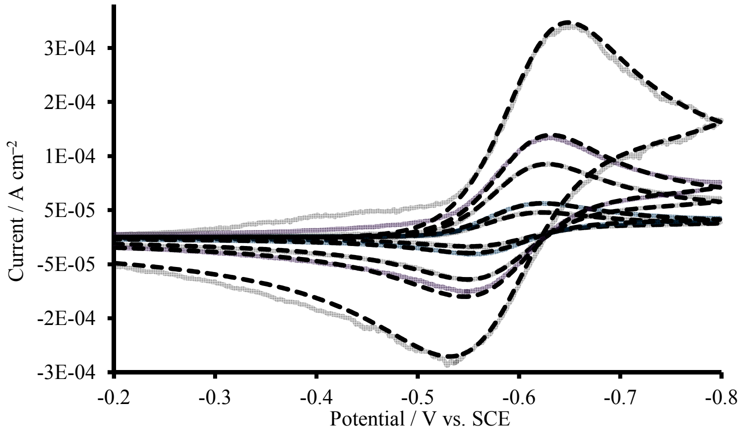

Fig. 4. Comparison of experimental (solid) and simulated (dash) CVs for the reduction of [py-H-py]$^+$ in aqueous solution at pH 5.2 using a 0.5 M KCl aqueous electrolyte, a polished Pt disk (0.13 cm^2) working electrode, a large area platinum counter electrode, and a SCE reference at scan rates: 5, 10, 50, 100 and 500 mV/s.

In addition to informing the understanding of pK$_a$s of key transient catalytic species in the pyridinium catalyzed reduction of CO_2, the Keith-Carter results have provided the finding that the calculated redox potential for the aqueous pyridinium/pyridinyl couple does not agree with the redox potential experimentally observed at a platinum electrode via cyclic voltammetry. This theoretical finding has been confirmed by several other theoretical groups (Lim, *et al.*, 2012; Etrem, *et.al.* 2013) using a variety of quantum chemical tools. The discrepancy is well outside the errors associated both with the experimental measurement (± 10 mV) or the calculated value (± 0.5 V). Thus, while the calculated pK$_a$s for a wide variety of pyridines and pyridinyl species (including 4,4'-bipyridine and pyridine) appear well aligned with experimental data, the redox potential for the simple pyridinium/pyridinyl couple yields a disagreement between experiment and quantum mechanical calculation. Based on the observed discrepancy, it can be concluded that there are chemical steps or, more specifically, a free energy term that is involved in the reduction of aqueous pyridinium that is not represented by the reaction scheme given in Eq. (1b). Keith and Carter (Keith and Carter, 2012) and separately Lim and Musgrave (Lim, *et al.*, 2012) have suggested that the missing free energy might be associated with surface adsorption of pyridinium prior to its reduction: under this condition pyridinyl is not being formed under the pure solution homogenous conditions assumed in their calculation. This explanation, while definitely being a key process in the overall pyridinium catalyzed reduction of CO_2 to organics as we previously noted (Cole *et al.*, 2010), and quite possibly weakly occurring in association with the reduction of pyridinium, is not evidenced by cyclic voltammetric or rotating disk electrode studies. This puts an upper energy boundary on the process that is far below that needed to induce a ~1 V potential shift. Importantly, our calculations, using the Keith-Carter approach, indicate that the hydrogen bonded dimer has a calculated redox potential that is very similar to pyridinium itself. Thus, the existence of the dimer as the redox active species does not explain the apparent discrepancy.

Though noted by Keith and Carter, what has been overlooked in this discussion is the implication associated with the necessity to invoke a tightly coupled hydrogen evolution reaction, such as reaction (3) in fitting of cyclic voltammetric data obtained in the absence of CO_2. Previously, we reported (Cole *et al.*, 2010), that without explicitly requiring a strong coupling between reaction 1(b) and hydrogen evolution via an EC' mechanism, one cannot obtain a satisfactory simulation of the cyclic voltammetric data for aqueous pyridinium reduction at a platinum electrode. This result echoes earlier literature that first postulated reaction (4) and reported that the reduction of pyridinium in nonaqueous electrolyte leads to H_2 evolution (Baumgartel *et al.*, 1984).

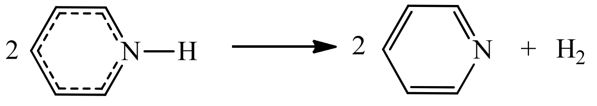

(4)

Scheme 4.

In our prior studies, we experimentally determined the rate constant for the hydrogen evolution reaction to be ~3 M^{-1}s^{-1} under our reaction conditions, while the heterogeneous charge transfer given by Eq. 1(b) has a much higher rate, typified by a zero field, heterogeneous charge transfer rate constant, k°, of 0.010 cm/s (Cole *et al.*, 2010). Thus, in this reaction sequence the formation of H_2 is rate limiting and the net reaction is:

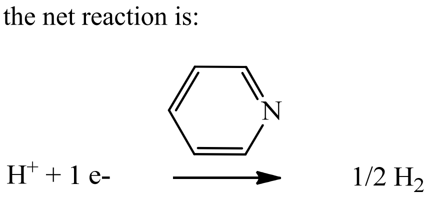

(5)

Scheme 5.

which, under the chemical conditions employed in our experiments (i.e., pH = 5.2, 1 atm H_2) is expected to occur thermodynamically at –0.55 V vs. SCE by a direct application of the Nernst equation. This redox potential is, in fact, what is experimentally observed within the expected experimental

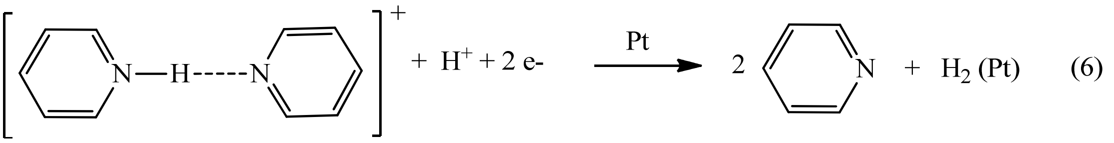

Scheme 6.

error. The level of coupling needed to make Eq. (3) mechanistically controlling cannot be obtained by a simple sequential reaction mechanism [1(a) → 2(b) → (3)] occurring in homogeneous solution. Further, we and Keith have separately noted that the observed reactivity is highly dependent on the electrode material employed, precisely following the hydrogen overpotential of the electrode (Cole *et al.*, 2010). Thus, the net reaction is unlikely to be a purely homogeneous process. This conclusion is supported by an independent theoretical investigation on a platinum surface (Etrem *et al.*, 2013) in which, through an inner sphere charge transfer, the redox potential for direct proton reduction from the pyridinium N-H via formation of a platinum hydride was calculated to be ca. –0.7 V vs. SCE. This potential is within the range of expected error. Therefore, it is likely that reaction (3) when carried out in aqueous electrolyte is better represented by a surface mediated process. Alternately hydrogen formation might occur via a proton coupled charge transfer reaction (PCET) (Scheme 6).

In this latter case, proton reduction and the coupling of the putative "hydrogen atom" must effectively occur on the electrode surface, thus providing an explanation for the direct relationship between electrode hydrogen over potential and the ability to reduce aqueous pyridinium. For these reasons, along with the fact that a PCET reaction singularly provides the tight mechanistic coupling between reaction 1(b) and hydrogen evolution needed to shift the system's redox potential to the observed value, reaction (6) is the mechanistically preferred route. In theory, the distinction between reaction step (4) and (6) should be observable via the concentration dependence of the reaction; however, the complexity of the reaction sequence along with the observed concentration saturation (Morris *et al.*, 2011) associated with a surface adsorption step, make this analysis highly ambiguous.

CONCLUSIONS

A full consideration of the overall thermochemistry associated with aqueous pyridinium reduction at a platinum electrode explains why the reported quantum chemical calculations did not reproduce the actual experimental data. In reaching this finding, we have identified a hydrogen bonded pyridinium-pyridine dimer as the most likely redox active species in the reduction of aqueous pyridinium. We will report in the future on the fate of the reduced pyridine dimer system in the presence of CO_2.

ACKNOWLEDGMENTS

This manuscript is based upon work supported by the Air Force Office of Scientific Research under AFOSR Award No. FA9550-10-1-0572 and the National Science Foundation under Award No. CHE-0911114. Dr. Yong Yan and Prof. Andrew Bocarsly thank Prof. Emily Carter and Dr. John Keith for helpful discussions. Crystallography facility manager Dr. Phil Jeffrey is acknowledged for his help refining the structure presented here.

REFERENCES

Albo, A., Luis, P. and Irabin, A. (2010). Carbon Dioxide Capture from Flue Gases Using a Cross-Flow Membrane Contactor and the Ionic Liquid 1-Ethyl-3-methylimidazolium Ethylsulfate. *Ind. Eng. Chem. Res.* 49: 11045–11051.

Amyes, T.L., Diver, S.T., Richard, J.P., Rivas, F.M. and Toth, K. (2004). Formation and Stability of N-Heterocyclic Carbenes in Water: The Carbon Acid pK_a of Imidazolium Cations in Aqueous Solution. *J. Am. Chem. Soc.* 126: 4366−4374.

Aresta, M. (2010). *Carbon Dioxide as Chemical Feedstock*, Wiley-VCH Verlag GmbH & Co., Weinheim.

Barton, E.E., Rampulla, D.M. and Bocarsly, A.B. (2008). Selective Solar-driven Reduction of CO_2 to Methanol Using a Catalyzed p-GaP Based Photoelectrochemical Cell. *J. Am. Chem. Soc.* 130: 6342–6345.

Baumgartel, H. and Retzlav, K.J. (1984). In *Encyclopedia of Electrochemistry of the Elements*; Bard, A.J. and Lund, H. (Eds.), Marcel Dekker, New York, NY, 15: 194.

Bocarsly, A.B., Gibson, Q.D., Morris, A.J., L'Esperance, R.P., Detweiler, Z.M., Lakkaraju, P.S., Zeitler, E.L. and Shaw, T.W. (2012). Comparative Study of Imidazole and Pyridine Catalyzed Reduction of Carbon Dioxide at Illuminated Iron Pyrite Electrodes. *ACS Catal.* 2: 1684–1692.

Brammer, L. and Zhao, D. (1995). Low-Temperature Structures of $[py_2H]^+[Co(CO)_4]^-$ (py = Pyridine) and $[(tmen)H]^+[Co(CO)_4]^-$ (tmen = *N,N,N',N'*-Tetramethylethylenediamine). *Acta Cryst.* C51: 45–48.

Cole, E.B., Lakkaraju, P.S., Rampulla, D.M., Morris, A.J., Abelev, E. and Bocarsly, A.B. (2010). Using a One-Electron Shuttle for the Multielectron Reduction of CO_2 to Methanol: Kinetic, Mechanistic, and Structural Insights. *J. Am. Chem. Soc.* 132: 11539–11551.

Emsley, J. (1980). Very Strong Hydrogen Bonding. *Chem. Soc. Rev.* 9: 91–124

Ertem, M.Z., Konezny, S.J., Araujo, C.M. and Batista, V.S. (2013). Functional Role of Pyridinium during Aqueous Electrochemical Reduction of CO_2 on Pt(111). *J. Phys. Chem. Lett.* 4: 745–748.

Glidewell, C. and Holden, H.D. (1982). Structure of Bis(4-methylpyridine)hydrogen(I) Tetraphenylborate. *Acta Cryst.* B38: 667–669.

Hamiliton, W.C. and Ibers, J.A. (1968). Hydrogen Bonding in Solids; W. A. Benjamin, New York.

Keets, K., Morris, A., Zeitler, E., Lakkaraju, P. and Bocarsly, A. (2010). In *Solar Hydrogen and Nanotechnology V*, 7770, Idriss, H. and Wang, H. (Eds.), SPIE, San Diego, CA.

Keith, J.A. and Carter, E.A. (2012). Theoretical Insights into Pyridinium-Based Photoelectrocatalytic Reduction of CO_2. *J. Am. Chem. Soc.* 134: 7580–7583.

Lim, C., Holder, A.M. and Musgrave, C.B. (2013). Mechanism of Homogeneous Reduction of CO_2 by Pyridine: Proton Relay in Aqueous Solvent and Aromatic Stabilization. *J. Am. Chem. Soc.* 135: 142–154.

Minshall, P.C. and Sheldrick, G.M. (1978). Pyridinium 2,2, 5,5-tetrathio-*cyclo*-di(phosphadithianate), $[(\text{pyridine})_2H]_2^{2+}$ $[P_2S_8]^{2-}$. *Acta Cryst.* B34: 1378–1380.

Morris, A.J., McGibbon, R.T. and Bocarsly, A.B. (2011). Electrocatalytic Carbon Dioxide Activation: The Rate-Determining Step of Pyridinium-Catalyzed CO_2 Reduction. *Chemsuschem* 4: 191–196.

National Oceanic & Atmospheric Administration (NOAA) – Earth System Research Laboratory (ESRL), Trends in Carbon Dioxide Values Given are Dry Air Mole Fractions Expressed in Parts Per Million (ppm). http://www.esrl.noaa.gov/gmd/ccgg/trends/#mlo (Website Accessed on June 26, 2013).

Schah-Mohammedi, P., Shenderovich, I.G., Detering, C., Limbach, H.H., Tolstoy, P.M., Smirnov, S.N., Denisov, G.S. and Golubev, N.S. (2000). Hydrogen/Deuterium-Isotope Effects on NMR Chemical Shifts and Symmetry of Homoconjugated Hydrogen-Bonded Ions in Polar Solution. *J. Am. Chem. Soc.* 122: 12878–12879.

Seshadri, G., Lin, C. and Bocarsly, A.B. (1994). A New Homogeneous Electrocatalyst for the Reduction of Carbon Dioxide to Methanol at Low Overpotential. *J. Electroanal. Chem.* 372: 145–150.

Tayyari, S.F., Mahdizadeh, S.J., Holakoei, S. and Wang, Y.A. (2010). Vibrational Assignment and Proton Tunneling in Pyridine–pyridinium Complexes. *J. Mol. Struct.* 971: 39–43.

Yan, Y., Zeitler, E.L., Gu, J., Hu, Y. and Bocarsly, A.B. (2013). Electrochemistry of Aqueous Pyridinium: Exploration of a Key Aspect of Electrocatalytic Reduction of CO_2 to Methanol. *J. Am. Chem. Soc.* 135: 14020–14023.

Received for review, June 29, 2013
Accepted, August 27, 2013